

# **SANDIA REPORT**

SAND2017-5599

Unlimited Release

Printed Month and Year

## **QUICKLOOK OVERVIEW OF MODEL CHANGES IN MELCOR 2.2: Rev 6342 to Rev 9496**

Larry L. Humphries

Prepared by  
Sandia National Laboratories  
Albuquerque, New Mexico 87185 and Livermore, California 94550

Sandia National Laboratories is a multi-mission laboratory managed and operated by Sandia Corporation, a wholly owned subsidiary of Lockheed Martin Corporation, for the U.S. Department of Energy's National Nuclear Security Administration under contract DE-AC04-94AL85000.

Approved for public release; further dissemination unlimited.



**Sandia National Laboratories**

Issued by Sandia National Laboratories, operated for the United States Department of Energy by Sandia Corporation.

**NOTICE:** This report was prepared as an account of work sponsored by an agency of the United States Government. Neither the United States Government, nor any agency thereof, nor any of their employees, nor any of their contractors, subcontractors, or their employees, make any warranty, express or implied, or assume any legal liability or responsibility for the accuracy, completeness, or usefulness of any information, apparatus, product, or process disclosed, or represent that its use would not infringe privately owned rights. Reference herein to any specific commercial product, process, or service by trade name, trademark, manufacturer, or otherwise, does not necessarily constitute or imply its endorsement, recommendation, or favoring by the United States Government, any agency thereof, or any of their contractors or subcontractors. The views and opinions expressed herein do not necessarily state or reflect those of the United States Government, any agency thereof, or any of their contractors.

Printed in the United States of America. This report has been reproduced directly from the best available copy.

Available to DOE and DOE contractors from

U.S. Department of Energy  
Office of Scientific and Technical Information  
P.O. Box 62  
Oak Ridge, TN 37831

Telephone: (865) 576-8401  
Facsimile: (865) 576-5728  
E-Mail: [reports@osti.gov](mailto:reports@osti.gov)  
Online ordering: <http://www.osti.gov/scitech>

Available to the public from

U.S. Department of Commerce  
National Technical Information Service  
5301 Shawnee Rd  
Alexandria, VA 22312

Telephone: (800) 553-6847  
Facsimile: (703) 605-6900  
E-Mail: [orders@ntis.gov](mailto:orders@ntis.gov)  
Online order: <http://www.ntis.gov/search>



SAND2017-5599  
Unlimited Release  
Printed Month Year

# **QUICKLOOK OVERVIEW OF MODEL CHANGES IN MELCOR 2.2: Rev 6342 to Rev 9496**

Larry L. Humphries  
Severe Accident Analysis Department  
Sandia National Laboratories  
P.O. Box 5800  
Albuquerque, New Mexico 87185-0748

## **Abstract**

MELCOR 2.2 is a significant official release of the MELCOR code with many new models and model improvements. This report provides the code user with a quick review and characterization of new models added, changes to existing models, the effect of code changes during this code development cycle (rev 6342 to rev 9496), a preview of validation results with this code version. More detailed information is found in the code Subversion logs as well as the User Guide and Reference Manuals.





# CONTENTS

1.	INTRODUCTION.....	9
2.	MELCOR Code DEVELOPMENT AND IMPROVEMENTS .....	10
2.1	New Defaults .....	10
2.1.1	Fuel Rod Collapse Model .....	10
2.1.2	Melt Spreading in Cavity .....	10
2.1.3	Sensitivity coefficients.....	10
2.2	Significant code corrections since revision 6342 .....	11
2.2.1	Mass error with flashing model when hygroscopic model is enabled [r8612] .....	11
2.2.2	Corrections to reflood quench model [multiple revisions] .....	11
2.2.3	Lipinski dryout model not used above the core support plate [r7874] .....	12
2.2.4	Revised candling model for canisters [r7864 but not active until 9387] .....	12
2.2.5	Decay heat transfer to small fluid volumes [r8274] .....	12
2.2.6	Correction to fuel rod collapse modeling (temperature failure criteria) [r8574] .....	12
2.3	New or Extended Modeling.....	12
2.3.1	COR Heat Transfer Paths Extended to Heat Structures [r6354] .....	12
2.3.2	Homologous pump model [r7205].....	12
2.3.3	Multi-HS radiation enclosure model [r7227, 8572] .....	13
2.3.4	Aerosol re-suspension model [r7095, r7315] .....	13
2.3.5	Zukauskas heat transfer coefficient (external cross-flow across a tube bundle) [r6945, r7641].....	13
2.3.6	Heavy reflector model [r7105, 7790] .....	13
2.3.7	Core Catcher (multiple containment vessels) [r7234, r8561].....	13
2.3.8	Multiple fuel rod types in a COR cell [r7515, r8572] .....	14
2.3.9	Generalized Fission Product Release Model [r7197] .....	14
2.3.10	New debris cooling models added to CAV package [r7108] .....	14
2.3.11	Spreading model implemented into CAV package [r5291, r8445] .....	15
2.3.12	Improvements to the CND package to allow multiple PCCS and ICS models [r6519, r7293].....	15
2.3.13	Turbulent Deposition Modeling [r3296, r6854, r8262].....	15
2.3.14	Temporal Relaxation Models [r7271, r8264] .....	15
2.3.15	Vectorized control functions [r8036, ongoing] .....	16
2.4	Minor Code Improvements.....	16
2.4.1	Control Functions .....	16
2.4.2	Output .....	16
2.5	MELCOR Dashboard Beta Release.....	17
3.	Changes in Predicted Results. ....	18
4.	Validation Cases.....	23
4.1	Hygroscopic Model .....	23
4.2	Oxidation Models .....	24
5.	Numerical Variance.....	26
6.	References .....	29

## FIGURES

Figure 1. Hydrogen generation by code revision (rev 8000 – rev 8700).....	20
Figure 2. Hydrogen generation by code revision (rev 9220 – rev 9496).....	20
Figure 3. AHMED Experiments (82% RH) .....	23
Figure 4. FPT-1 Hydrogen Generation from Oxidation .....	24
Figure 5. CORA-13 Hydrogen Generation from Oxidation .....	25
Figure 6. Quench-6 Hydrogen Generation from Oxidation.....	25
Figure 7 - Cumulative distribution function for the total hydrogen mass generated from oxidation. ....	26
Figure 8 Cumulative distribution function for the CPU time. ....	27

## TABLES

Table 1. Mapping of model changes to revision number	21
--	----

## NOMENCLATURE

BWR	Boiling Water Reactor
CAV	Cavity (package)
CCI	Core Concrete Interaction
CF	Control Function (package)
CND	Condenser
COR	Core (package)
CPU	Central Processing Unit
CV	Control Volume
DOE	Department of Energy
FPT	Fission Product Test
HR	Heavy Reflector
ICS	Isolation Condenser System
LHC	Lower Head Containment (package)
MCCI	Molten Core Concrete Interaction
OECD	Organization of Economic Cooperation and Development
PCCS	Passive Containment Cooling System
PWR	Pressurized Water Reactor
RN	RadioNuclide (package)
SNL	Sandia National Laboratories
TP	Transfer Process (package)
SOARCA	State Of the Art Reactor Consequence Analysis



## **1. INTRODUCTION**

MELCOR is a fully integrated, engineering-level computer code designed to analyze severe accidents in nuclear power plants and nuclear fuel cycle facilities. Created at Sandia National Laboratories for the U.S. Nuclear Regulatory Commission (NRC), MELCOR's primary purpose is to model the progression of accidents in light water reactor nuclear power plants. Development of MELCOR was motivated by Wash1400<sup>1</sup>, a reactor safety study produced for the NRC, and the Three Mile Island nuclear power plant accident. Since the project began in 1982, MELCOR has undergone continuous development to address emerging issues, process new experimental information, and create a repository of knowledge on severe accident phenomena.

MELCOR 2.2 is a significant official release of the MELCOR code with many new models and model improvements. This report provides the code user with a quick review and characterization of new models added, changes to existing models, the effect of code changes during this code development cycle (rev 6342 to rev 9496), and a preview of validation results with this code version. The user is referred to the MELCOR User Guide<sup>2</sup> and Reference Manual<sup>3</sup> to provide clarification of existing code parameters or models.

## 2. MELCOR CODE DEVELOPMENT AND IMPROVEMENTS

### 2.1 New Defaults

#### 2.1.1 *Fuel Rod Collapse Model*

MELCOR has long had a time-at-temperature model for determining the collapse of fuel rods but it has not been the default behavior and the time-at-temperature characteristics had to be provided by the user. By default, rods will collapse based on a temperature failure criteria. Such a criteria leads to a threshold effect that leads to numerical variance in calculations since failure of a ring of rods, a catastrophic degradation event, is highly sensitive to the maximum clad temperature that is calculated. The time-at-temperature characteristics are based on experimental observations from the VERCORS experiments together with SOARCA models as derived from Phebus experience and were derived by Denman<sup>4</sup>.

#### 2.1.2 *Melt Spreading in Cavity*

A new melt spread model for debris in the cavity has been added and is now the default. Previously, debris would immediately spread across the floor unless a control function was provided to specify a user-defined spreading rate.

#### 2.1.3 *Sensitivity coefficients*

SC1260(6) was added for the precursor heat transfer coefficient, HTCPRE, used in the revised reflood quench model described further below and in the UG/RM.

SC1270 - Default values for the pool-bridging model parameters were adjusted based on observed behavior over a wider range of problem conditions. The default for 1270(1) the minimum pool fraction for bridging, lower was changed from 0.1 to 0.6. The default for 1270(2) the minimum pool fraction for bridging, upper was changed from 0.001 to 0.1.

SC1505(1) (PMNBLK) was changed to 1.e-5. This fixes an inconsistency in the PM Darcy law modeling which can cause numerical problem when small fluid volume is left in an area full of debris.

SC4408(1) - The default value was changed from 1000000 to 1001000, disabling the add-hoc model that redefines old velocities that was introduced in an attempt to improve behavior by preserving the old volume flow as the void fraction changes during the iteration.

SC7001 – The aerosol coefficient relative error was changed from 1.0E-3 to 1.0E-6 in order to reduce a mass conservation error in radionuclide classes. This sensitivity coefficient is used as a convergence test for a numerical integration for aerosol coefficients. Typically these coefficients are calculated once at the start of a calculation. However, if this sensitivity coefficient is modified in a MELCOR input, the aerosol coefficients are re-evaluated using this new value.

SC7106 - A discrepancy between the default release rate model for cesium and the final SOARCA best practices<sup>5</sup> was observed. The SOARCA best practice values predict a faster release rate, particularly at lower temperatures. In revision 8596, sensitivity coefficients 7106 were modified to be consistent with the final SOARCA best practice report.

SC	Description	Old Default	Rev 8596
C7106(1,1)	Diffusion coefficient for low burnup	2.3e-9	1.0e-6
C7106(2,1)	Diffusion coefficient for high burnup	2.3e-9	1.0e-6
C7106(4,1)	Activation energy	2.41e5	3.814e5
C7106(1,2)	Diffusion coefficient for low burnup (alternate)	5.0e-8	1.0e-6
C7106(2,2)	Diffusion coefficient for high burnup (alternate)	2.5e-7	1.0e-6
C7106(4,2)	Activation energy (alternate)	3.8e-7	3.814e5

## 2.2 Significant code corrections since revision 6342

A number of code corrections have been made since the last official code release. Some of the more important ones are outlined here.

### 2.2.1 Mass error with flashing model when hygroscopic model is enabled [r8612]

A mass error that was originally attributed to the hygroscopic model was traced to the flashing model, when the hygroscopic model was enabled ([Bug 279](#), [Bug 608](#), [Bug 1760](#)). The error occurred because the flashing model predicts the fog produced (per unit volume) within a flow path. Then during the CVH/FL advection step, this mass of steam is advected (added) to the downstream control volume. However, in a later subroutine, the mass distribution of fog in the Rosin-Rammler distribution predicted by the flashing routine is placed in the RN aerosol mass. In the case of the hygroscopic model, this means that the fog mass is added twice, once as aerosol mass and once as CVH mass. The code was modified to reduce the CVH mass advected by the fog flashing mass.

### 2.2.2 Corrections to reflood quench model [multiple revisions]

Several model corrections and numerical improvements to how MELCOR treats quenching were developed and implemented that have significantly improved the robustness of the code for reflood conditions. To prevent unphysical pressure oscillations, one set (1) temporally relaxes the rate-of-change of the quench velocity and (2) causes the quench velocity to be smoothly driven to zero within a small user-specified distance of the pool level. Another important correction fixed an inconsistency in the DTDZ model so that it now uses the “unquenched T<sub>hot</sub>” temperature instead of average component temperature for heat transfer between the core component and the Atm. Finally, when the quench front and the Pool level are not equal and the Pool is subcooled, the heat transfer from the hot core structure to the pool in this region is now partitioned between a direct vaporization part and a pool-heatup part to account for vapor bubble collapse in the subcooled pool.

### *2.2.3 Lipinski dryout model not used above the core support plate [r7874]*

The Lipinski dryout model was intended for limiting the heat removal from a debris bed with downward flowing coolant to capture the case where dryout occurs and the downward flow of water is counter-balanced by the upward flow of steam. This model was also applied above the core support plate with upward flow of coolant and would lead to problems when the occurrence of particulate debris along with intact components would stop convective heat removal from the intact components in a COR cell.

### *2.2.4 Revised candling model for canisters [r7864 but not active until 9387]*

According to MELCOR candling logic, molten metallic zircalloy from canister rubble would candle onto intact rods, leading to oxidation of clad and fuel rod failure. It is physically more appropriate that melt from the canister rubble should candle onto the canisters instead of fuel rods.

### *2.2.5 Decay heat transfer to small fluid volumes [r8274]*

This error involved the transfer of a fraction of the decay heat to the fluid volume even when the fluid volume becomes infinitesimally small. The solution was to dial back the decay heat transfer to the fluid volumes as this volume becomes small. This is accomplished by linearly reducing the fraction of the decay heat energy to zero, starting when the porosity drops below the maximum of 0.01 and PMNSRF (SC1505(2)) and is completely zero when the porosity (fluid volume) is zero.

### *2.2.6 Correction to fuel rod collapse modeling (temperature failure criteria) [r8574]*

It was noted that on occasion fuel rods would continue to stand up to 3100 K even though the failure temperature, TRDFAI, was 2500.0 K by default. A logic in implementing the time-at-temperature fuel rod collapse model was responsible and would ignore the TRDFAI criteria when the clad metal mass thickness was less than 0.1 mm.

## **2.3 New or Extended Modeling**

Several models have been added to the code or extended to satisfy user needs.

### *2.3.1 COR Heat Transfer Paths Extended to Heat Structures [r6354]*

This feature has been extended to allow specification of a heat transfer path from a COR component to a heat structure. The heat transfer path must be defined 'From' a valid COR component and the heat structure must not have a user specified boundary condition (i.e., IBCL = 0,20,30,80, or 90). Furthermore, if a radiation path is defined, the emissivity must be defined by the user on the appropriate HS Boundary Surface Radiation Data record (HS\_LBR or HS\_RBR).

### *2.3.2 Homologous pump model [r7205]*

The new MELCOR homologous pump model is similar to that of RELAP (RELAP5-3D, RELAP4) but with some distinguishing features. Several new MELGEN input records have been added that, in general, allow the user to fully specify 1) rated pump conditions, 2) single/two-phase pump performance via homologous curve input, 3) pump friction torque as a polynomial, 4) pump inertia as a polynomial, 5) pump speed and motor torque controls, and 6) pump trips. Additionally, pump data from the Semiscale and Loft experiments is available as a “built-in” option and a “universal correlation” taken from the literature is included.

### ***2.3.3 Multi-HS radiation enclosure model [r7227, 8572]***

A radiation enclosure consists of two or more surfaces that envelope a region of space for which radiation transfer occurs among those surfaces. The space between these surfaces may or may not be filled with a participating medium, for which the gas may absorb, emit, and scatter radiation emitted by the surfaces. Each surface is assumed to be isothermal, opaque, diffuse, and gray, and are characterized by uniform radiosity.

### ***2.3.4 Aerosol re-suspension model [r7095, r7315]***

A new resuspension model was incorporated into MELCOR<sup>6</sup>. The model is for resuspending deposited aerosol from inside a pipe due to rapid gas flow through the pipe that dislodges particles. The model approach is based on the force balance method, in which a deposited particle is lifted off if the aerodynamic disturbing force is greater than the adhesive force/

### ***2.3.5 Zukauskas heat transfer coefficient<sup>7</sup> (external cross-flow across a tube bundle) [r6945, r7641]***

The Zukauskas correlation for external cross-flow across a tube bundle has been added as an option for the HS boundary surface data records (HS\_LB – left, and HS\_RB – right). This empirical correlation has been developed for both staggered and aligned tube arrays relative to the fluid velocity vector and has been applied to a helical coil steam generator design.

### ***2.3.6 Heavy reflector model [r7105, 7790]***

In general, the heavy reflector (HR) lies between the reactor core and the core barrel and is a new component available to the PWR-HR reactor type. Acting as a shield for the core barrel, the HR experiences the heating due to absorption of the radiation from the fission power. To avoid overheating and melting, the heat is removed from the water flowing through a large number of channels drilled through the HR. In general, channels with a number of orifices are used to calibrate the flow in each channel by varying the resistances. In addition, there is a small gap between HR and the core barrel, which allows very small flow between them. The HR component resides in the outer active core ring for the PWR-HR.

### ***2.3.7 Core Catcher (multiple containment vessels) [r7234, r8561]***

A new ‘LHC’ (Lower Head and Containment) package has been added to MELCOR to model a “second lower head” or a “core-catcher” structure around/about the COR lower head. This new model calculates the thermal response of a new LHC structure and debris supported by this

structure. The user specifies the LHC plate geometry, material, nodalization, etc. as well as CVH connections and COR/RN interfaces via TP. The following functionality is expected for this LHC package (items in red are still in development).

1. Receive debris (mass, energy) and RN inventory via TP upon COR LH failure
2. Predict various energy exchanges between debris, CV, and LHC structure
3. Predict attending debris phase changes
4. Predict LHC structural failure (mechanisms similar to COR lower head)
5. Predict debris relocation to CAV
6. Relocation of debris to multiple LHC structures.
7. Debris metal oxidation by steam/water, multi-LHC (like CAV)

#### *2.3.8 Multiple fuel rod types in a COR cell [r7515, r8572]*

In modeling the Sandia PWR spent fuel pool experiment it became apparent that in order to capture the steep temperature gradient at the rack boundary it was necessary to represent the bundle with multiple rod types with independent temperatures<sup>8</sup>. This temperature gradient was essential in predicting the timing of propagation of ignition from one fuel rod to the next. The multi-rod model adds additional rod types that the user can utilize to represent the fuel rods within a core cell. Each rod type has a fraction of the fuel rod mass and surface area associated with those rods and the user specifies radiation view factors for radiation heat transfer. Each rod type can candle independently, oxidize independently, and will satisfy failure criteria independently. However, currently when one rod type in a cell fails, all other rod type components will fail simultaneously, even though those other rod types may not have reached a failure criteria. This model has been implemented for the PWR spent fuel reactor type and the PWR reactor type only.

#### *2.3.9 Generalized Fission Product Release Model [r7197]*

A generalized fission product release model has been added to MELCOR consisting of two components, a burst fission product release term and a cumulative diffusive fission product release term.

#### *2.3.10 New debris cooling models added to CAV package [r7108]*

Recent MELCOR code development has focused on improvements to the ex-vessel core-melt cooling models available to MELCOR code users. In particular, a water ingress model, a melt eruption model, and a melt spreading model were added in MELCOR code revision 7108 (water ingress) and revision 7483 (melt spread) and have been available in all subsequent interim code releases.

##### **2.3.10.1 Water-ingression**

The water ingress model implemented in MELCOR is based on the model by Epstein and generally follows the implementation in CORQUENCH. This model allows water in the crust layer if the upper heat flux is less than a dryout flux. The water ingress model was assessed

internally against the CCI experiments (performed under the OECD MCCI project). This model is intended to replace best practices involving multiplication factors for thermal conductivity and boiling terms based on assessment against the Argonne National Laboratory tests.

#### **2.3.10.2 Melt eruption through crust**

The melt eruption model is implemented in the MELCOR CAV package as a transfer of mass from the melt layer into the debris layer, where the rate of transfer is proportional to the gas sparging rate. This relocated debris has an associated porosity and is therefore more coolable, where the permeability is based on the dryout flux.

#### ***2.3.11 Spreading model implemented into CAV package [r5291, r8445]***

The spreading model implemented in MELCOR is based on a balance between gravitational and viscous forces. The new Ramacciotti model for the enhancement to the debris viscosity for two-phase (solid/liquid) flow has been implemented. This model was adopted from the MELTSPREAD code of ANL and was assessed against the Vulcano VE-U7 test. Prior to this model, melt would spread across the cavity in a single time step by default, or would spread at a parametric rate specified by the user through a control function.

#### ***2.3.12 Improvements to the CND package to allow multiple PCCS and ICS models [r6519, r7293]***

The improvements to this package were to accommodate multiple ICS and PCCS objects. Otherwise, the modeling for individual CND objects are identical to the previous implementation.

One slight modeling variation was to allow the user to specify the variation of the capacity with various containment conditions using the MELCOR control functions. Previously, the user specified a tabular function which was used to calculate the variation locally in the CND subroutines. However, control functions are evaluated only at the end of the calculation and not locally in the CND subroutines. This can lead to slightly different results since the tabular function approach might tend to be more implicit. As another option available to the modeler, the TF package was modified to allow the user to specify a control function for the Y value for each X-Y data pair.

#### ***2.3.13 Turbulent Deposition Modeling [r3296, r6854, r8262]***

The input has been restructured since the original implementation and now utilizes optional string input to provide a more readable input deck. In addition, the user can specify a flow path for determining the flow velocity. In the previous release, the flow velocity was obtained from the CV velocity. Finally, the text output has been enhanced to report tabulated results for the turbulent deposition.

#### ***2.3.14 Temporal Relaxation Models [r7271, r8264]***

Many physical processes in MELCOR are modeled by correlation based relationships developed from steady-state experiments. These models do not represent the time it takes for these processes to respond if conditions change. As a result, temporal “rate-of-change” aspects of MELCOR simulations are not expected to be highly accurate and numerical instabilities can be magnified when sudden changes occur. Temporal relaxation is a simple way to introduce a user-imposed time-scale based model that limits how quickly processes being modeled can change in time.

### ***2.3.15 Vectorized control functions [r8036, ongoing]***

The control function package has been extended to allow control functions to return a vector of results and to receive vectors of input to include vectorized control function arguments. The ‘RANGE’ construct has been added which defines a list of objects (control volumes, COR cells, heat structures, etc.) with a particular order associated with those objects. Vectorized control function arguments can refer to ranges and existing control function types have been modified to operate on vector control function arguments. Finally, an analytic function has been created which is a user programmed function that receives and returns vectors and is compiled into a library that MELCOR can then call.

## **2.4 Minor Code Improvements**

### ***2.4.1 Control Functions***

Control functions arguments added to the plot file now have units associated with the plot file where before control functions in the plot file were not given units.

New real-valued (CF-CONST) and logical constant (CF-LCONST) control function arguments have been added.

By default, all control functions are added to the plot file. A new record, CF\_PLOT, allows the user to omit selected control functions from the plot file.

### ***2.4.2 Output***

When a user generates HTML output for a MELCOR run for a PWR reactor type, bitmaps showing the core degradation state, temperature contours, oxidation rate, and ZR mas are embedded on the HTML output for each output time.



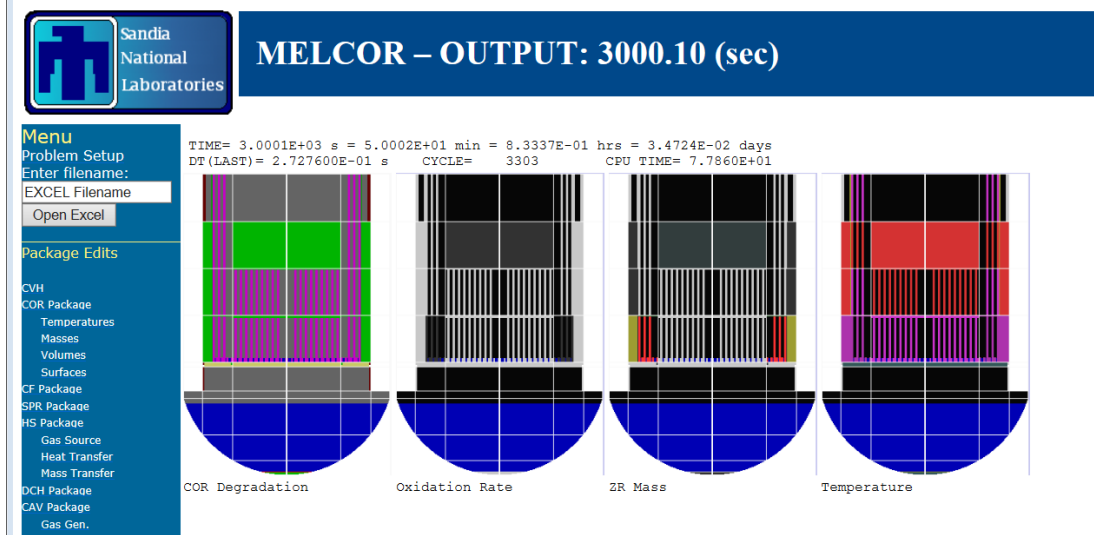


Figure 1. Screen shot of HTML output showing COR degradation bitmaps.

## 2.5 Changes to simple PWR and BWR Demo Input Decks

## 2.6 MELCOR Dashboard Beta Release

MELCOR Dashboard is a quickwin version of the MELCOR executable that can be used for monitoring the status of a MELCOR calculation as it is running. Because this utility is interactive, it has access to the entire MELCOR database as the calculation is running, making it possible to visualize greater detail in the calculation than might be available from the binary plotfile. In addition, mass and energy balances are monitored and there are visualizations for core degradation, oxidation, etc., aerosol components, deposition, heat structure temperature profiles, etc. Further, users can monitor control functions and the data is available at every time step rather than just at plot intervals. This tool is available only as a beta release at this time and comments/suggestions are welcome, but it is not fully supported at this time.

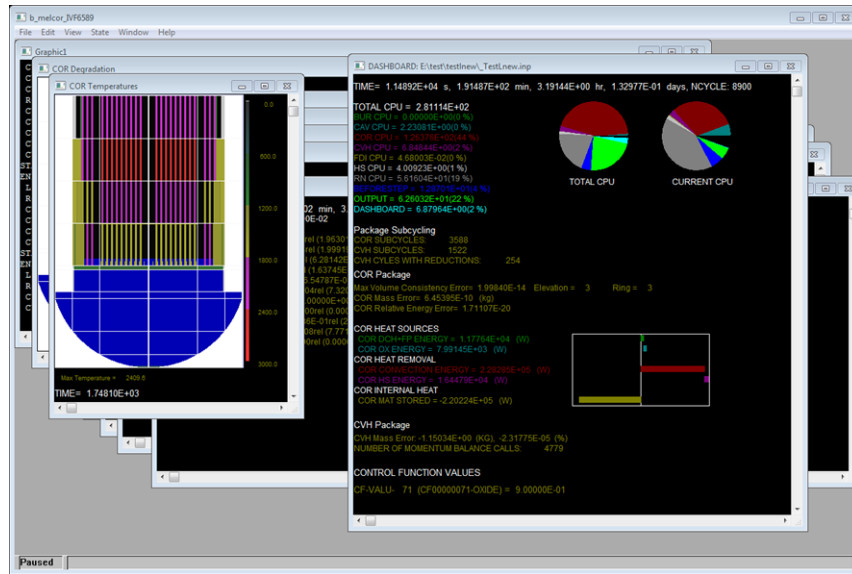


Figure 2. Screenshot of MELCOR Dashboard Display.

### 3. CHANGES IN PREDICTED RESULTS.

The simple demonstration input decks (PWR and BWR) that are provided with each MELCOR download were run with each code revision to assess changes for important calculated metrics. In particular, the hydrogen mass generated for each case is reported here for each code revision. This metric is affected by in-vessel phenomena resulting from core heat up, relocation, oxidation, and boil-off and provides an important indication of differences in calculation results. Since these are very simple input decks with extremely coarse nodalization, the sensitivity of this parameter may be expected to be larger than what might be observed in an actual plant deck but they do demonstrate the sensitivity to individual corrections to the code. A plot is provided over the entire range of revisions in this code release (r6342 to r9496) in Figure 3 as well as plots over smaller ranges in Figures through Figure 7. In Figure 3 the data points for some revisions are modified to identify those revisions related to a particular physics model. As pointed out earlier in this document, significant improvements were made to the reflood quench model over an extended period of development. Table 1 identifies important revisions where results were observed to change and maps them to physics models in the code. A more complete description of these revisions can also be found in the Subversion logs that are provided with the M2.2 code release.

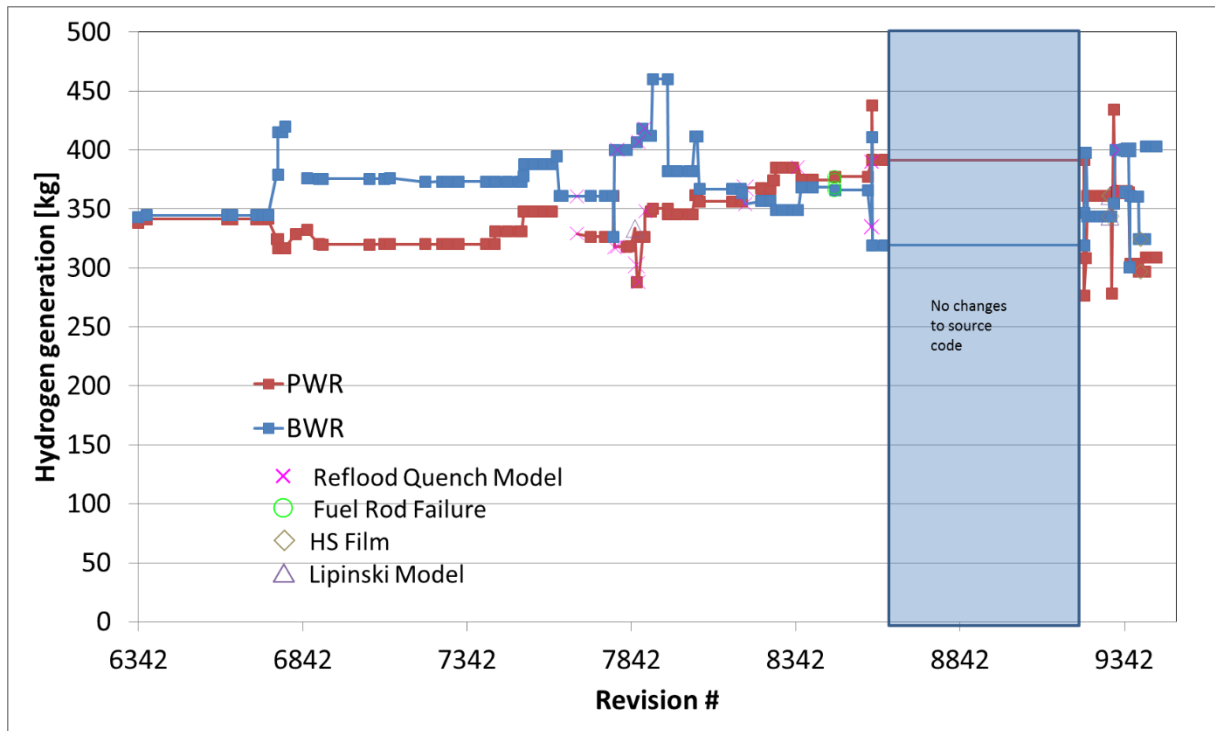


Figure 3 Hydrogen generation by code revision (rev 6342 – rev 9496).

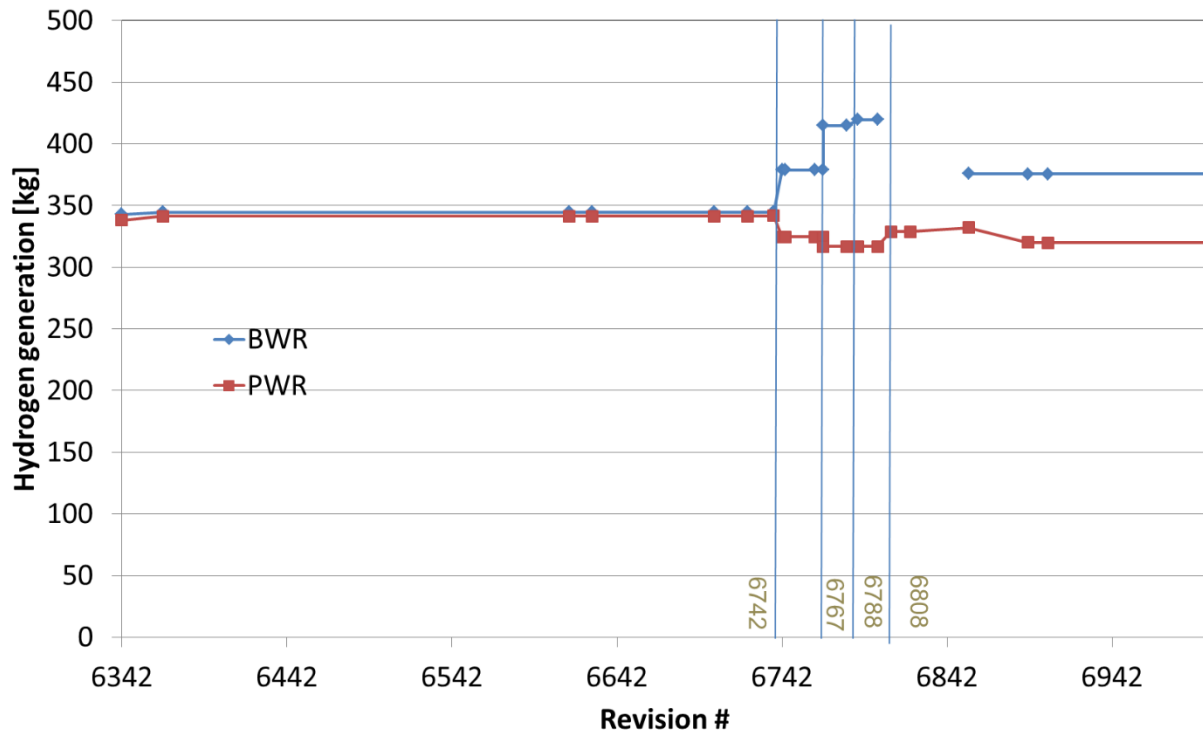


Figure 4. Hydrogen generation by code revision (rev 6342 – rev 7000).

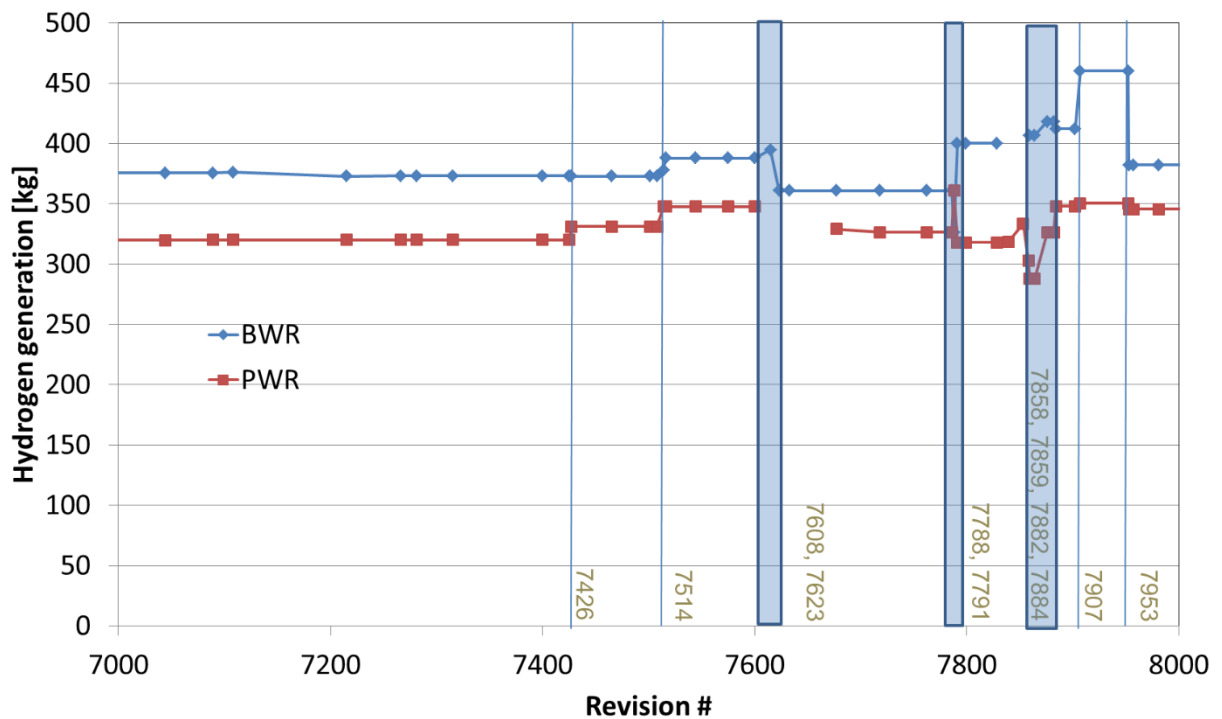


Figure 5. Hydrogen generation by code revision (rev 7000 – rev 8000).

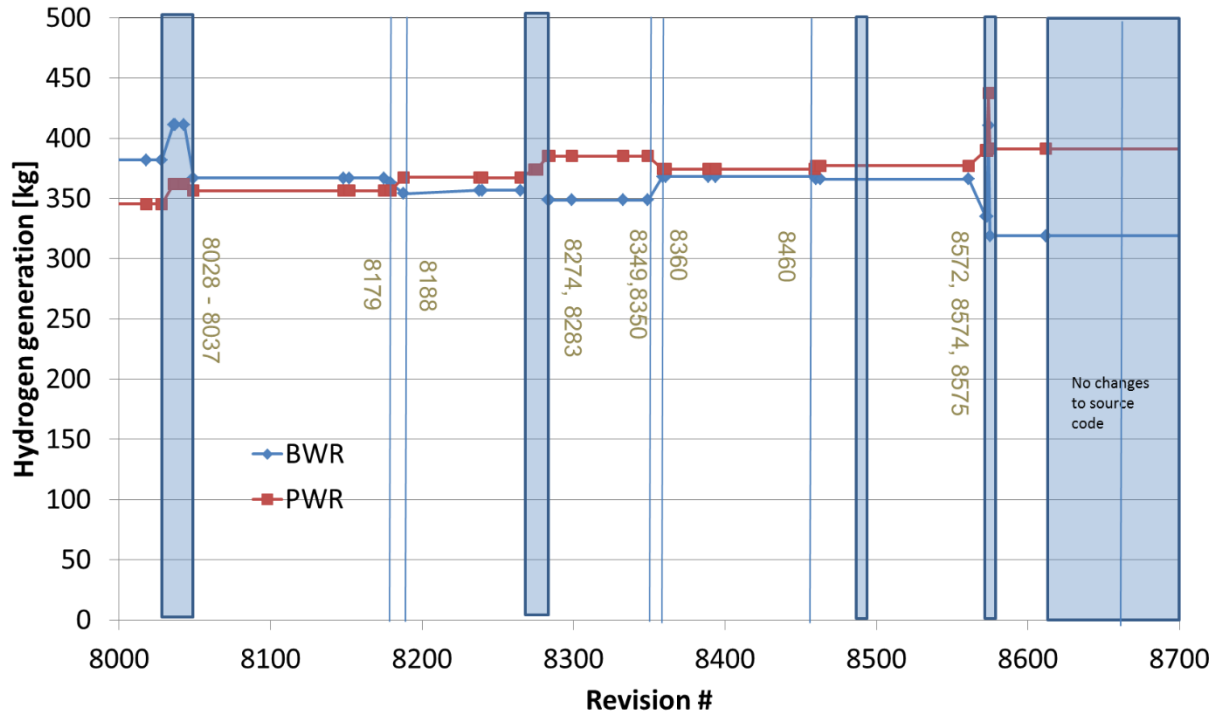


Figure 6. Hydrogen generation by code revision (rev 8000 – rev 8700).

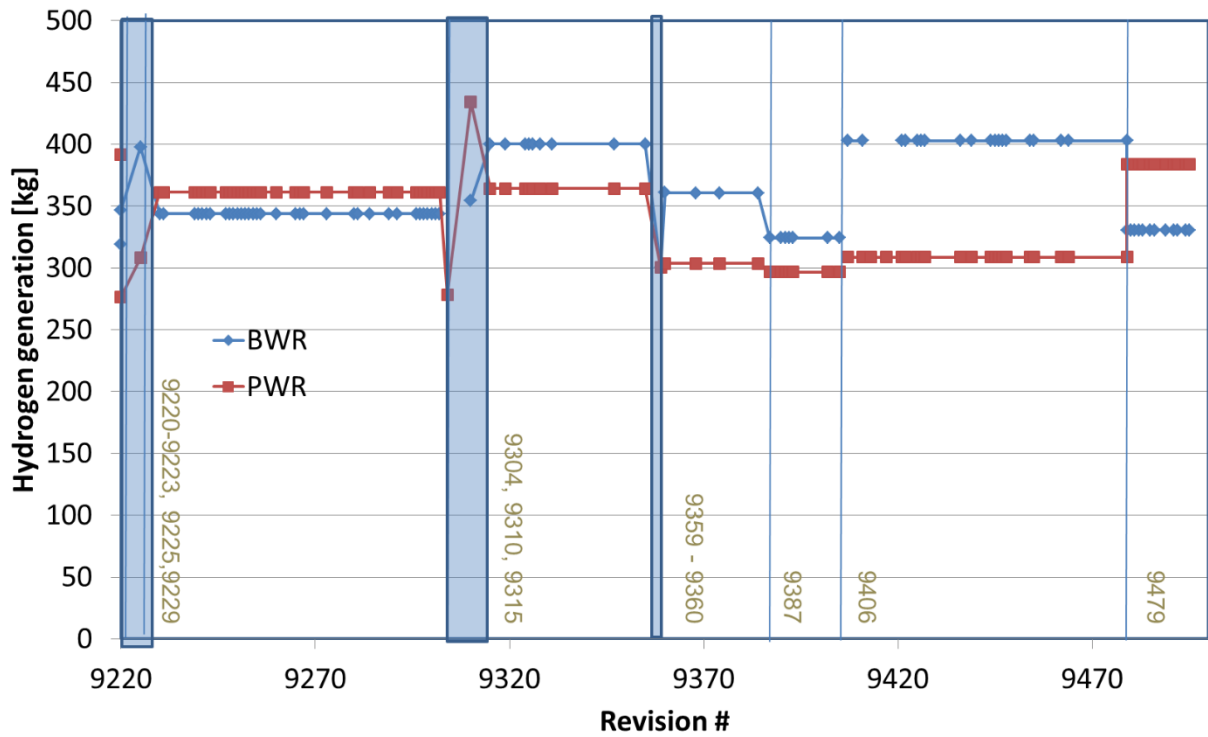


Figure 7. Hydrogen generation by code revision (rev 9220 – rev 9496).

**Table 1. Mapping of model changes to revision number**

Revision	Fuel Rod Failure	Quench Related	DTDZ Related	HS Film	Lipinski Model	Roundoff	Other
6614							
6626							
6699							
6767							Molten Pool model
6788						x	COR subgrid model
6820							
6903							
6939							
7108							
7426							Molten pool model
7608							degassing model
7623							film drainage
7791		x					
7858		x					
7859		x					
7882					Δ		
7884		x					
7907		x					
7953		x					
8028 - 8036	Can't build over this range and can't identify which revision is responsible (likely 8035)						
8049							void fractions in tiny pools
8179						x	Movement of small masses
8188							
8274			x				Decay heat transfer to small volumes
8283		x					
8349			x				
8350			x				
8460		x					
8572							
8574	○						Fuel Collapse Model
8575	○						Time-at-temperature rod collapse
9220		x					
9221		x					
9222							
9223							Bubble release model

9225		x					
9229							Small fluid volume
9304				✱			
9310					△		
9315				✱			
9359		x					
9360		x					
9387	□						BWR Candling Logic
9406				✱			
9479						x	MAEROS convergence

## 4. VALIDATION CASES

The MELCOR validation report<sup>9</sup> has not been updated at this time but will be at a later date. Even so, preliminary results are provided here to help the code user understand the impact that recent modeling changes might have on validation cases. A number of code corrections have been made that affect specific models such as the hygroscopic and reflood quench models. Consequently, changes in validation tests that assess these models are of particular interest. In addition, other code changes can effect core degradation or heat transfer and hence, oxidation and generation of hydrogen. Plots from several validation tests are provided to demonstrate that the code continues to provide reasonable agreement with validation experiments.

### 4.1 Hygroscopic Model

Several changes have been made to the hygroscopic model in this code release. Revisions 9445 and 9446 changed the precision of a variable used for testing convergence to double precision to correct a runtime convergence error. Further, revision 8611 corrected a mass conservation error that occurred when both the hygroscopic and flow path flashing model were enabled simultaneously. Even with these model corrections, the AHMED tests demonstrate that this model was not adversely effected by these changes. Other code changes were made to correct a mass conservation error that was observed when the hygroscopic model and the flow path flashing model are active. However, this is not a subject of any of the existing validation cases.

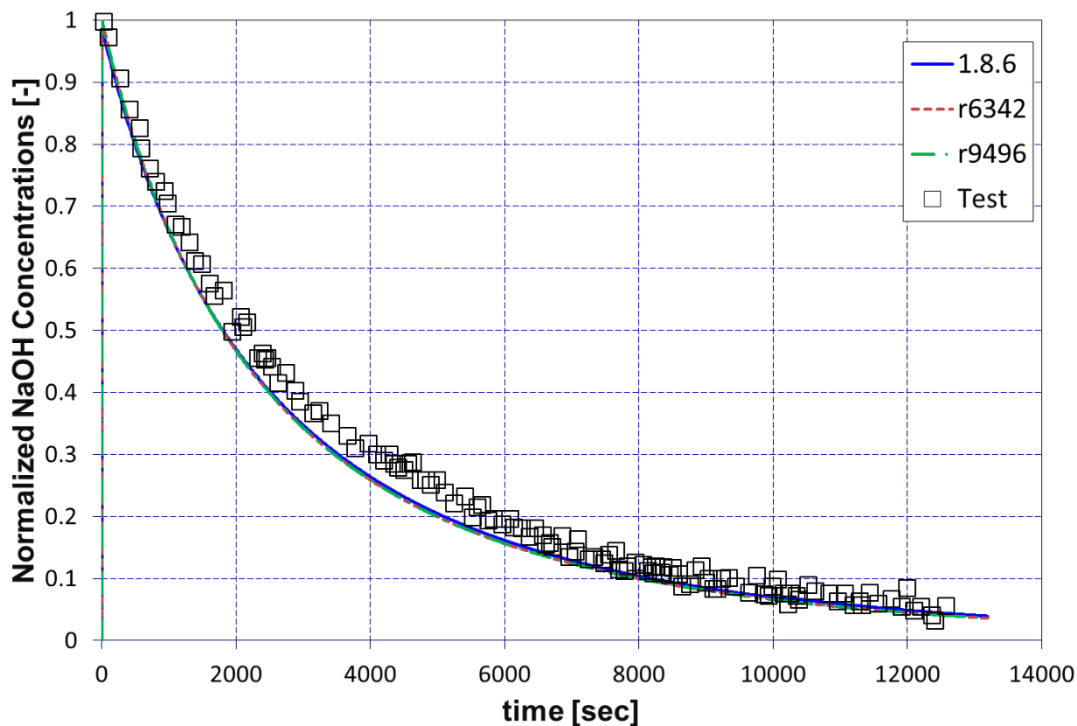
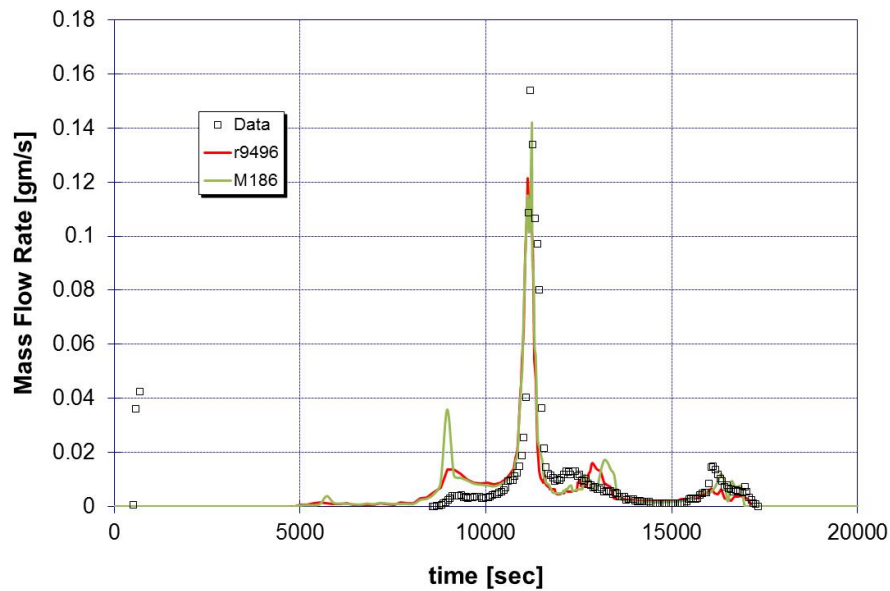


Figure 8. AHMED Experiments (82% RH) comparison with MELCOR 1.8.6, MELCOR 2.1 (r6342) and MELCOR 2.2 (r9496).



## 4.2 Oxidation Models

A number of code corrections addressed the reflood quench model which effects component surface temperatures and hence oxidation rates. In addition, many changes can have an impact on core degradation, which can also affect surface areas available for oxidation. No changes were made directly to the oxidation rate modeling during this development cycle. The plots below demonstrate that oxidation is still well-predicted for the FPT-1, CORA-13, and quench-6 tests.



**Figure 9. FPT-1 Hydrogen Generation from Oxidation**

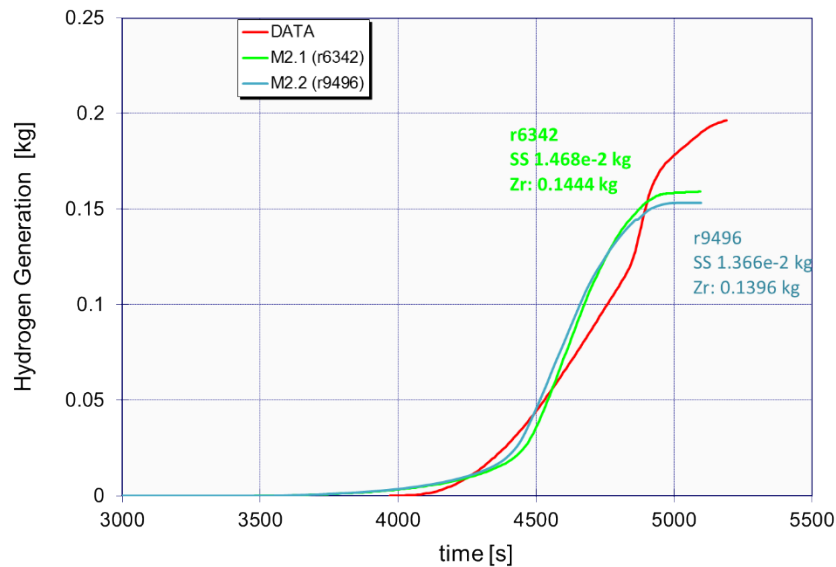


**Figure 10. CORA-13 Hydrogen Generation from Oxidation**

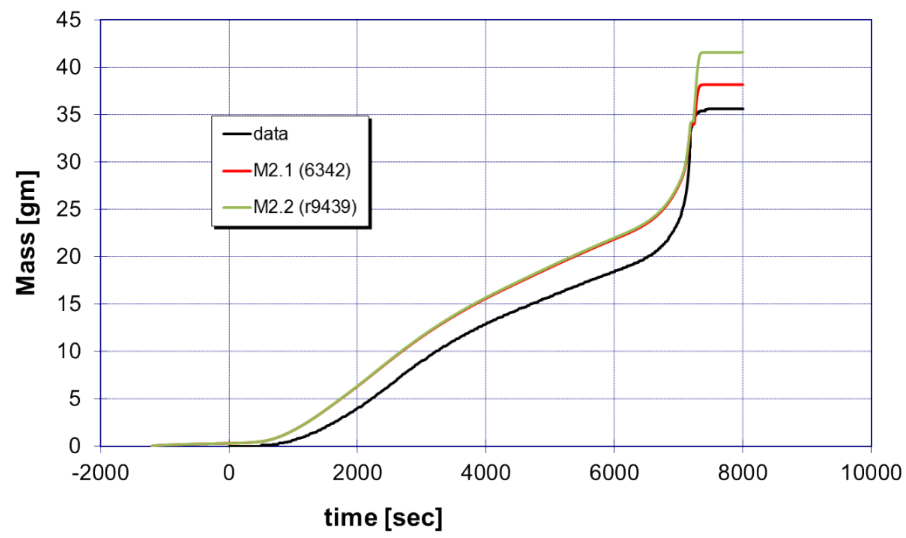


**Figure 11. Quench-6 Hydrogen Generation from Oxidation**

## 5. NUMERICAL VARIANCE

MELCOR, and other codes like it, have always had sensitivity to various sources leading to perturbations in results and users have long been aware that changing the time step that MELCOR takes can lead to variances in calculated parameters. Most recently it has become apparent to users of MELCOR 2.1 that changing the order of flow paths in a deck (flow path shuffling) can lead to perturbations. However, this was also true of MELCOR 1.8.6 (and other codes) but largely went unnoticed because the flow paths were pre-sorted by number during problem setup. The flow path ordering provides a source of noise in the solution due to differences in the matrix solve for the flow calculation. This source can then be amplified by various physics models and bifurcations in accident scenario paths, etc. Here we perform a random flow path reordering on a Fukushima unit1 input deck and from it find the numerical variance in several parameters, hydrogen mass generated and CPU. Our intention is to reduce this numerical variance through smoothing of models and so it is important to track this parameter over time and these plots will provide a baseline for future code development. MELCOR was modified in revision 6440 to allow random re-ordering of the flow path order to provide an initiator for monitoring numerical variance.

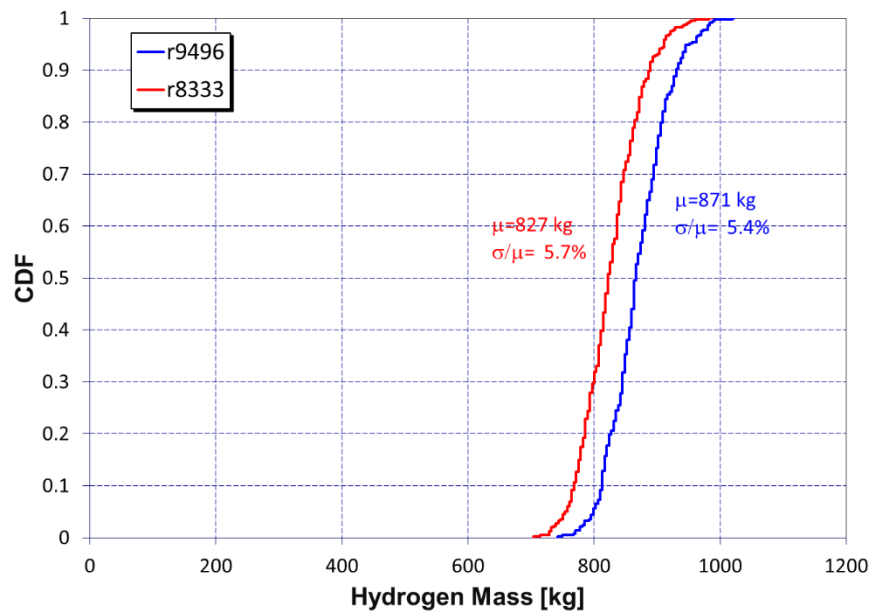


**Figure 12 - Cumulative distribution function for the total hydrogen mass generated from oxidation.**

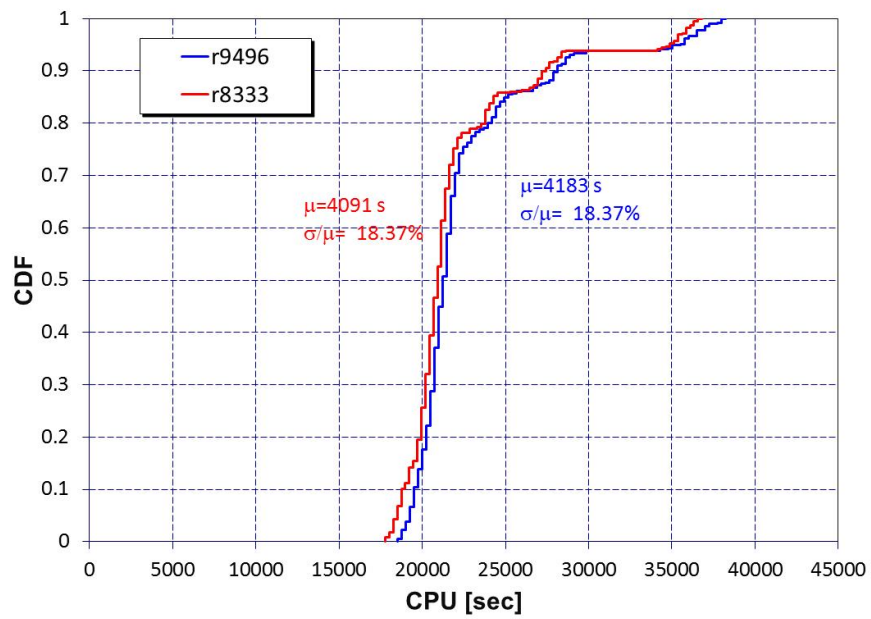


**Figure 13 Cumulative distribution function for the CPU time.**



## 6. REFERENCES

- 1 Bartel, Reynold, “WASH-1400 – The Reactor Safety Study – The Introduction of Risk Assessment to the Regulation of Nuclear Reactors,” NUREG/KM-0010, Office of Nuclear Regulatory Research, USNRC, August 2016.
- 2 Humphries, L.L., Cole, K.K., Louie, D.L., Figueroa, V.G. and Young, M.F., MELCOR Computer Code Manuals- Vol.1: MELCOR Primer and Users Guide, Version 2.1 6840 2015, SAND2015-6691 R, Sandia National Laboratories, Albuquerque, NM, August 2015.
- 3 Humphries, L.L., Cole, K.K., Louie, D.L., Figueroa, V.G. and Young, M.F., MELCOR Computer Code Manuals- Vol.2: MELCOR Reference Manual, Version 2.1 6840 2015, SAND2015-6691 R, Sandia National Laboratories, Albuquerque, NM, August 2015.
4. Denman, et al., “Fukushima Daiichi Unit 1 Uncertainty Analysis – Exploration of Core Melt Progression Uncertain Parameters – Volume II”, SAND2015-6612, Sandia National Laboratories, Albuquerque, NM, 2015
- 5 Ross, Kyle, et al., “MELCOR Best Practices as Applied in the State-of-the-Art Reactor Consequence Analyses (SOARCA) Project,” NUREG/CR-7008, United States Nuclear Regulatory Commission, August 2014.
- 6 Young, “Liftoff Model for MELCOR,” SAND2015-6119, Sandia National Laboratories, Albuquerque, NM, July 2015.
- 7 Incropera, F.P., Dewitt, D.P., Bergman, T.L., and Lavine, A.S. Fundamentals of Heat and Mass Transfer, 6th Edition. John Wiley & Sons, Inc., Hoboken, NJ, 2007.
- 8 Durbin, et al., “Spent Fuel Pool Project Phase II: Pre-Ignition and Ignition Testing of a Commercial 17x17 Pressurized Water Reactor Spent Fuel Assembly under Complete Loss of Coolant Accident Conditions,” Sandia National Laboratories, June 2014.
- 9 Humphries, et al., “MELCOR Computer Code Manuals, Volume 3: MELCOR Assessment Problems,” SAND2015-6693, Sandia National Laboratories, Albuquerque, NM, August 2015.